

1 Development of an objective index, neural activity score (NAS), reveals neural network ontogeny and
2 treatment effects on microelectrode arrays

3 Short title: Objective quantification of neural networks on MEAs

4

5 Austin P. Passaro^{1,2}, Onur Aydin³, M. Taher A. Saif³, Steven L. Stice^{1,2*}

6

7

8 ¹Regenerative Bioscience Center, University of Georgia, Athens, Georgia, United States of America

9 ²Biomedical Health and Sciences Institute, Division of Neuroscience, University of Georgia, Athens,
10 Georgia, United States of America

11 ³Department of Mechanical Science and Engineering, University of Illinois at Urbana-Champaign,
12 Urbana, IL

13

14 * Corresponding author

15 E-mail: ssstice@uga.edu

16

17 Author contributions: Conceptualization, A.P.P. and S.L.S.; Data Curation, A.P.P.; Formal Analysis,
18 A.P.P.; Funding Acquisition, S.L.S.; Investigation, A.P.P. and O.A.; Methodology, A.P.P., O.A.,
19 M.T.A.S., and S.L.S.; Project Administration, A.P.P. and S.L.S.; Resources, A.P.P., O.A., M.T.A.S., and
20 S.L.S.; Software, A.P.P.; Supervision, M.T.A.S. and S.L.S.; Validation, A.P.P. and O.A.; Visualization,
21 A.P.P.; Writing – Original Draft Preparation, A.P.P. and S.L.S.; Writing – Review & Editing, A.P.P.,
22 O.A., M.T.A.S., and S.L.S.

23 **Abstract**

24 Microelectrode arrays (MEAs) are valuable tools for electrophysiological analysis at a cellular population
25 level, providing assessment of neural network health and development. Analysis can be complex,
26 however, requiring intensive processing of large high-dimensional data sets consisting of many activity
27 parameters. As a result, valuable information is lost, as studies subjectively report relatively few metrics
28 in the interest of simplicity and clarity.

29 From a screening perspective, many groups report simple overall activity; we are more interested in
30 culture health and changes in network connectivity that may not be evident from basic activity
31 parameters. For example, general changes in overall firing rate – the most commonly reported parameter
32 – provide no information on network development or burst character, which could change independently.
33 Our goal was to develop a fast objective process to capture most, if not all, the valuable information
34 gained when using MEAs in neural development and toxicity studies.

35 We implemented principal component analysis (PCA) to reduce the high dimensionality of MEA data.
36 Upon analysis, we found that the first principal component was strongly correlated to time, representing
37 neural culture development; therefore, factor loadings were used to create a single index score – named
38 neural activity score (NAS) – reflective of neural maturation. To validate this score, we applied it to
39 studies analyzing various treatments. In all cases, NAS accurately recapitulated expected results,
40 suggesting this method is viable. This approach may be improved with larger training data sets and can be
41 shared with other researchers using MEAs to analyze complicated treatment effects and multicellular
42 interactions.

43

44

45

46 **Author Summary**

47 Analyzing neural activity has important applications such as basic neuroscience research, understanding
48 neurological diseases, drug development, and toxicity screening. Technology for recording neural activity
49 continues to develop, producing large data sets that provide complex information about neuronal function.
50 One specific technology, microelectrode arrays (MEAs), has recently given researchers the ability to
51 record developing neural networks with potential to provide valuable insight into developmental
52 processes and pathological conditions. However, the complex data generated by these systems can be
53 challenging to analyze objectively and quantitatively, hindering the potential of MEAs, especially for
54 high-throughput approaches, such as drug development and toxicity screening, which require quick,
55 simple, and accurate quantification. Therefore, we have developed an index for simple quantification and
56 evaluation of neural network maturation and the effects of perturbation. We present validation of our
57 approach using several treatments and culture conditions, as well as a meta-analysis of toxicological
58 screening data to compare our approach to current methods. In addition to providing a simple
59 quantification method for neural network activity in various conditions, our method provides potential for
60 improved results interpretation in toxicity screening and drug development.

61

62 **Introduction**

63 Micro- (or multi-)electrode arrays (MEAs) are valuable tools for network-level electrophysiological
64 analysis of neuronal populations [1–4]. While sacrificing single cell resolution compared to traditional
65 patch clamp electrophysiology, MEAs allow for recordings of entire neural networks both *in vitro* and *in*
66 *vivo* and can be used to study dynamic network properties and development, either spontaneously or in
67 response to stimulation or treatment. During recording, action potentials, or spikes, are detected *via*
68 recording the corresponding voltage changes in the extracellular environment. Analysis of spike patterns
69 provides network characteristics such as firing rate and network synchrony (see S1 Table) for list of all
70 measured parameters), which are useful when determining neuronal network function and/or response to
71 perturbation (*i.e.* stimulation or pharmacological treatment) [5,6].

72 Given these advantages, along with the advent of multi-well MEA plates that allow for higher-throughput
73 screening and more complex experimental design, MEAs have seen widespread adoption from
74 characterizing neural maturation to toxicity screening and drug development. Interestingly, despite the
75 adoption of MEAs for these screening approaches, analysis has typically been limited to mean firing rate
76 and other metrics of overall activity [7,8]. This limited analysis severely underutilizes MEA capabilities
77 and may result in “false-negative” screening results, as only conditions or compounds that increase or
78 decrease overall neural activity will be registered as hits with no regard to other aspects of neural network
79 functionality or ontogeny. Current MEA analysis methods require the use of raster plots to visualize
80 network development or individual parameter analysis, which are qualitative and difficult to interpret,
81 respectively. While a general pattern of network development from sporadic spikes to sporadic bursts to
82 coordinated synchronous network bursts has been well-described in previous studies [2,3,9,10], there is
83 currently a lack of sufficient methods to quantify this observed ontogeny.

84 Here, we developed a method implementing dimensionality reduction techniques, specifically principal
85 component analysis (PCA), to create a singular index score – named neural activity score (NAS) –

86 reflective of neural network ontogeny. NAS serves as an easily interpretable measurement to evaluate
87 spontaneous network development in simple and complex cultures (*i.e.* neuron-glia co-cultures) or effects
88 of various treatments (*i.e.* soluble factors or stimulation). We present validation of this method in several
89 experiments, including a culture media comparison, various conditioned media treatments, and a
90 microglia-neuron co-culture system, demonstrating the ability to measure both positive and negative
91 effects on neural network activity and further interrogate toxicological screening, evaluating sensitivity on
92 potential toxic compounds.

93

94 **Results**

95 **Neural network ontogeny revealed by microelectrode array**

96 Mouse embryonic stem cells were cultured and differentiated, resulting in cultures containing a mixture
97 of motor neurons, excitatory and inhibitory neurons, and glial cells [11]. These neural cultures were
98 allowed to mature on 48-well MEA plates over a 19-day period, typical for neuron maturation and
99 network formation for these cells [12]. Activity was detected at approximately 5 days post-seeding (days
100 *in vitro*; DIV) and increased gradually until reaching a plateau over the last several days of recording (16-
101 19 DIV). Qualitatively, raster plots generated at various time points throughout the recording period
102 demonstrate an expected pattern of network development: sparse and sporadic spikes appearing first,
103 followed by sporadic bursts, followed eventually by synchronous network bursts (Fig 1A-F). While this
104 emergent development is evident from the raster plots, it is difficult to quantify. Quantification of several
105 spike, burst, and network/synchrony metrics reveals general increases over time in these categories (Fig
106 1G-N), but current MEA analysis methods do not allow for simple quantification of network ontogeny
107 incorporating these and other activity metrics.

108 **Principal component analysis of MEA parameters reveals temporal correlation, allowing** 109 **for neural activity score derivation**

110 Given the complexity and multivariate nature of the data, PCA was performed to reduce dimensionality
111 and allow for easier visualization. After standard score normalization, all of the aforementioned
112 parameters at all time points were included as data points for PCA. Examining the two-dimensional
113 projection of the first two principal components revealed a distinct pattern in the data (Fig 2A). Adding a
114 dimension of time (*via* colormap), this pattern was revealed to be a temporal separation of the data points,
115 especially along the first principal component. Statistically, linear regression analysis supported this
116 temporal component, as principal component 1 (PC1) is strongly correlated to time (Fig 2B; $R^2=0.5441$,
117 $p<0.0001$), indicating recapitulation of network ontogeny and maturation. After confirmation of this
118 relationship, factor loading values for PC1 were examined to determine which factors (MEA parameters)
119 contributed most strongly to this component. While substantial contributions were observed for many
120 parameters, the strongest metrics were burst percentage, network burst percentage, number of spikes per
121 burst, number of bursting electrodes, number of spikes per network burst, and synchrony index (Table 1).
122 Notably, mean firing rate, the most common parameter analyzed in MEA studies, was the 11th-strongest
123 contributor. Finally, these factor loading values were used to develop an individual index score – NAS
124 (Equation 1; see Methods). As NAS represents all aspects of neural network activity, it allows for
125 assessment of neuronal network ontogeny and evaluation of the effects of various perturbations, such as
126 stimulation, pharmacological treatment, or alternative culture conditions, which can typically be difficult
127 to analyze if various parameters do not exhibit unidirectional changes. Additionally, NAS reduces the
128 high variation often observed in individual MEA parameters, as evidenced by lower coefficient of
129 variation for 24/25 (96%) measured parameters (S1 Fig).

130

131

132 **Table 1. Factor loading values for principal components 1-5 for all MEA parameters analyzed.**

<i>Parameter</i>	<i>PC1</i>	<i>PC2</i>	<i>PC3</i>	<i>PC4</i>	<i>PC5</i>
Burst Percentage - Avg	0.938953	-0.21655	-0.09068	0.095365	-0.03905
Network Burst Percentage	0.930335	-0.16411	-0.03479	-0.00912	0.030603
Number of Spikes per Burst - Avg	0.927633	-0.07813	0.131878	0.180872	-0.20604
Number of Bursting Electrodes	0.924737	0.11382	-0.13932	-0.05683	-0.03851
Number of Spikes per Network Burst per Channel - Avg	0.916818	-0.09696	0.059892	-0.0695	-0.30286
Synchrony Index	0.91299	-0.25337	-0.09404	0.126219	-0.03106
Number of Spikes per Network Burst - Avg	0.90668	-0.14074	0.063698	-0.03136	-0.3157
ISI Coefficient of Variation - Avg	0.875459	-0.13787	-0.14411	0.203831	-0.09526
Area Under Normalized Cross-Correlation	0.866748	-0.32439	-0.0838	0.14749	-0.01187
Number of Elecs Participating in Burst - Avg	0.866593	0.127533	-0.16016	-0.10207	-0.04436
Mean Firing Rate (Hz)	0.787233	-0.09261	0.483835	-0.01736	0.111684
Network IBI Coefficient of Variation	0.739427	0.22799	-0.36458	-0.23674	0.12618
Burst Duration - Avg (s)	0.730618	0.521412	0.032794	0.197191	-0.12086
Normalized Duration IQR - Avg	0.707402	0.327012	-0.30471	0.026697	0.337296
IBI Coefficient of Variation - Avg	0.64845	0.459111	-0.30775	0.114136	0.20907
Network Normalized Duration IQR	0.613893	0.064961	-0.38534	-0.17934	0.144007

Area Under Cross-Correlation	0.606648	-0.40216	0.517657	0.237669	-0.14355
Burst Frequency - Avg (Hz)	0.592944	-0.04631	0.437397	0.034638	0.423479
Network Burst Frequency (Hz)	0.506543	-0.0198	0.364146	-0.01999	0.590348
Network Burst Duration - Avg (sec)	0.490791	0.412156	0.078862	-0.54881	-0.07344
Width at Half Height of Cross-Correlation	0.233083	0.626106	0.385101	-0.42764	-0.13819
Width at Half Height of Normalized Cross-Correlation	0.175127	0.727927	0.205821	-0.28793	-0.18294
Mean ISI within Burst – Avg	0.029257	0.891807	0.112554	0.360375	0.016162
Median ISI within Burst - Avg	-0.05205	0.881542	0.1378	0.359244	0.017994
Inter-Burst Interval - Avg (s)	-0.27591	0.571143	-0.11858	0.370944	-0.15048

133 Parameters sorted by descending PC1 loading value.

134

135 **Enhancement of neural network ontogeny is easily quantified via NAS**

136 Regression analysis served as initial support that NAS accurately measures neural network ontogeny, but
137 we also sought to experimentally validate NAS in several conditions to further confirm this recapitulation.
138 For initial validation, several experiments were performed to analyze enhanced neural network ontogeny
139 and activity in response to different conditions known to enhance neural activity – namely, optimized
140 culture media [13] and muscle-conditioned media treatment [14]. To examine the effects of optimized
141 culture media, mixed neural cultures (HBG3-derived) were grown on MEAs in two different media
142 conditions: DMEM/F12 & Neurobasal-based medium (DMNB) or BrainPhysTM-based medium (BP).
143 While DMNB has traditionally been widely used to culture HBG3-derived and other neural cell lines, BP
144 was developed for electrophysiological applications due to a more physiologically relevant formulation,
145 resulting in increased electrophysiological function of various cell lines [13]. However, BP has not been
146 evaluated on HBG3-derived neural cultures. In both DMNB and BP groups, the neurons began showing
147 activity at approximately day 5, increasing over 3 weeks, as expected; however, the cells cultured in BP
148 exhibited enhanced activity and network development, as indicated by the significantly higher NAS (Fig
149 3A; $p < 0.0001$, two-way repeated measures ANOVA).

150 To examine the effects of conditioned media on network ontogeny, mixed neural cells were treated with
151 muscle cell (C2C12)-conditioned media (CM), which has previously been shown to significantly
152 accelerate network activity and development [14]. Likewise, NAS analysis showed similar results and
153 provided simple quantification (Fig 3B; $p < 0.0001$, two-way repeated measures ANOVA) of this
154 accelerated network development.

155 **Disruption of neural network ontogeny is easily quantified via NAS**

156 In addition to measuring neural network activity enhancement, we also sought to validate NAS on more
157 complex culture conditions and for quantifying disruption of network activity. Microglia, the resident
158 immune cells of the central nervous system (CNS), are being increasingly implicated in

159 neurodegenerative diseases and have been shown to be neurotoxic in many conditions [15–18]; therefore,
160 we decided to explore co-culturing microglia with mixed neural cultures on MEAs. After allowing
161 neurons to become active over 10 days, BV2 cells, an immortalized mouse microglia cell line, were added
162 to the cultures at 8 different cell densities. We observed rapid disruption in network function in a clear
163 cell density-dependent manner, with higher numbers of microglia relative to the neuronal population
164 resulting in accelerated network disruption, as indicated by a decrease in NAS (Fig 4A; $p < 0.0001$, two-
165 way repeated measures ANOVA, Tukey's post-hoc test).

166 To examine whether this disruption is contact-dependent or the result of secreted factors, neural cultures
167 were treated with BV2-conditioned media at 10 days (similarly to the co-culture experiment described
168 above). Similar to the co-culture condition, BV2-conditioned media treatment also disrupted network
169 function (Fig 4B), suggesting a role for microglia-secreted factors in neural network disruption. To
170 examine whether this effect was exacerbated by microglial activation, BV2 cells were stimulated with
171 two concentrations of the pro-inflammatory endotoxin lipopolysaccharide (LPS; 10 ng/mL and 100
172 ng/mL) for 24 hours prior to conditioned media collection. LPS-stimulated BV2-conditioned media
173 disrupted network function in a concentration-dependent manner, with unstimulated BV2-conditioned
174 media causing significant disruption ($p < 0.0193$, two-way mixed model, Tukey's post-hoc test), followed
175 by 10 ng/mL LPS stimulation ($p = 0.0003$) and 100 ng/mL LPS stimulation ($p < 0.0001$), providing further
176 support for NAS as a viable method to quantify complex treatment effects and evaluate disruption of
177 electrophysiological function.

178 **NAS summarizes neural activity for neurotoxicology screening**

179 Advances in MEA technology [8,19] have led to adoption of MEAs for neurotoxicological screening [20]
180 Given the potential of NAS to consolidate many functional MEA parameters, we sought to determine its
181 applicability to neurotoxicity screening.

182 For this analysis, NAS values were calculated from MEA toxicity screening of 52 compounds from the
183 NTP or ToxCast libraries [21,22] (Fig 5A-C). In previous studies [21,22], the authors performed a
184 network formation assay (NFA) using primary cortical neurons, measuring 17 parameters of activity in
185 response to compound treatment over 12 days on MEAs to determine compound effects on network
186 formation. Additionally, viability testing was performed to measure cytotoxicity. For each of these assays,
187 EC_{50} values were determined for each compound. Here, we used NAS values to calculate and compare
188 EC_{50} values to individual MEA parameter EC_{50} values and cytotoxicity EC_{50} values (Fig 5D-F, S2 Table).
189 Of the 52 compounds we analyzed, 33 were found to have measurable effects in the network formation
190 assay (defined as a decrease in activity by 3X median absolute deviation from control) for at least one
191 activity parameter (though the specific parameter(s) differed among compounds), and 26 compounds
192 were found to have measurable cytotoxicity in the viability assay [21] (Fig 5G). Similarly, using NAS
193 EC_{50} values, we found 26/52 compounds (50%) affected neural activity (Fig 5G). For these compounds,
194 we compared the EC_{50} calculated from NAS to determine sensitivity compared to the average individual
195 MEA parameter EC_{50} values and cytotoxicity EC_{50} values. We found NAS to be more sensitive (lower
196 EC_{50}) than the average of all parameters for 16/26 compounds (61.5%) and more sensitive than the
197 average cytotoxicity EC_{50} for 18/26 compounds (69.2%) (Fig 5G, S2 Table).

198

199 **Discussion**

200 Advances in MEA technology, including multi-well MEA plates, incubated recording setups, and
201 constantly improving software, allow for higher throughput than previously possible [18,19], though
202 analysis has traditionally been limited to simple parameters, primarily mean firing rate. Only recently
203 have researchers begun incorporating advanced metrics of network activity in these screening approaches
204 [20–22]. These advanced metrics have provided researchers with tools to record from entire neuronal
205 populations and analyze complex neuronal network dynamics. Multi-well MEAs enable high-throughput

206 neuronal recordings, facilitating their adoption for drug/toxicity screening applications and evaluation of
207 complex culture conditions. However, the information that can be gleaned from MEAs has been
208 hampered by limited analytical methods and tools, as well as high variation. Here, we present a novel
209 method to overcome these limitations – development of an index, neural activity score, that incorporates
210 and consolidates traditional MEA measurements into a single quantitative value that can be used to
211 objectively evaluate neuronal network development and function across various culture conditions,
212 treatments, and neural cell sources. This is valuable not only for basic neuroscience research on neuronal
213 networks, but also translational research and preclinical studies.

214 The results presented here demonstrate the value of NAS to assess potential developmental neurotoxicity
215 (DNT) hazards, a field with a widely recognized need for more sensitive, less variable, and higher
216 throughput functional assays [21–24]. The mixed neural cultures used for NAS derivation and the primary
217 cultures analyzed in the network formation assay are both maturing networks, derived from embryonic
218 stem cells or isolated from neonatal rodents, respectively. As a result, NAS is well-suited for analysis of
219 maturing neural networks, as is necessary in DNT studies, covering a range from non-active to full
220 maturity, with synchronized network bursting. The application to developing networks from multiple cell
221 sources suggest NAS has substantial value for improving the use of MEAs for toxicity screening and drug
222 development.

223 As the concern over drug development costs continues to rise, scientists are noticing several recurring
224 problems, including the reproducibility crisis and inadequacies of current screening assays, *in vivo*
225 models, and other preclinical studies [25–27]. For neural assays, specifically, assays have traditionally
226 used simple endpoints such as viability and morphological analysis (*i.e.* neurite outgrowth) for screening,
227 primarily due to scalability [28]. However, electrophysiological endpoints are often more sensitive and
228 allow for assessment of electrophysiological toxicity, which involves separate – and highly time-sensitive
229 – mechanisms [8,29,30]. By improving result interpretation, NAS will facilitate incorporation of
230 functional measures into screening programs focused on cytotoxicity and morphology.

231 Index scoring has been used extensively in clinical settings and *in vivo*; for example, neurological deficits
232 in amyotrophic lateral sclerosis (ALS) and Parkinson's disease (PD) are assessed using the Revised ALS
233 Functional Rating Scale (ALSFRS-R) [31] and United Parkinson's Disease Rating Scale (UPDRS) [32],
234 respectively. Stroke severity is frequently measured using various scales (*i.e.* modified Rankin scale
235 (mRS) [33,34] and NIH stroke scale (NIHSS)) [35], and these have been shown to correlate strongly with
236 patient outcomes and be useful for therapeutic evaluation [34]. The simplified analytical pipeline
237 provided by these indices is vital to detecting effects (or lack thereof) in clinical and preclinical studies.
238 Due to this, a need has been recognized to develop multivariate approaches and index scores for *in vitro*
239 approaches, as well [36,37]. Similar analysis pipelines provided by index scores could be especially
240 valuable for screening assays, allowing for improved hit detection when screening potential
241 neurotoxicants or therapeutics. Several composite scores have been developed to condense information
242 from multiple toxicity assays for specific compound classes (*e.g.* endocrine disruptors, halogenated
243 aliphatics), previously [38,39]. Here, we developed NAS using a similar approach to condense the high-
244 dimensional data from MEA recordings into a single measurement with reduced variation that can be
245 used to easily and consistently evaluate compound effects on neural activity, as opposed to analyzing
246 many different parameters individually. This reduced variation and improved interpretation could help
247 identify and/or narrow down compounds to examine and develop further, saving time and money wasted
248 on poor candidate compounds. Likewise, improved *in vitro* studies could help reduce the necessity of *in*
249 *vivo* studies, which are expensive, time-consuming, and have ethical and practical concerns due to a
250 myriad of potential endpoint measurements and species differences that can contribute to high variability
251 and difficulty determining true treatment effects [40].

252 The validation studies presented here indicate that the NAS formula provides an easily interpretable
253 measure of neural network health/functionality and overall effects of perturbation. By compiling all MEA
254 metrics as opposed to individual metrics (*i.e.* mean firing rate), NAS represents all aspects of neural
255 network function, which can provide more consistent analysis and results interpretation/reporting.

256 Additionally, NAS has the potential to provide increased sensitivity over a collection of individual
257 parameters, as NAS was more sensitive than the individual parameter average for 61.5% of compounds.
258 This result was interesting, demonstrating the utility of implementing relative parameter weights. Since
259 NAS was derived from how all parameters contribute to development/maturation, this result indicates that
260 this approach may describe treatment effects in a more holistic manner than analysis of individual
261 parameters alone, which only describe certain aspects of activity. However, when specific parameters are
262 of interest, we suggest incorporating NAS as an additional metric for screening, not as a complete
263 replacement, as a summary statistic for electrophysiological function and neural network maturation.
264 Additionally, larger training data sets and/or other optimization may allow for improved sensitivity in the
265 future.

266 Two of the three compounds for which NAS was found to be most sensitive, MPP+ and picroxystrobin,
267 share similar toxic mechanisms, both inhibiting mitochondrial electron transport chain complexes [41,42].
268 While further research would be needed to determine if this is more than a coincidence, it does suggest
269 mitochondrial function as a sensitive predictor of neurodegeneration. This finding supports a wealth of
270 evidence linking mitochondrial dysfunction to neurodegenerative diseases, in some cases prior to
271 symptom onset and diagnosis [43–45]. Using NAS to analyze and compare various compound classes in
272 more detail may allow for deeper insight into toxicity mechanisms for different compound classes or
273 varying therapeutic potential in drug discovery studies.

274 Lastly, challenges in analyzing complex and large data sets have been widely acknowledged across
275 multiple assays and techniques, including high-throughput screening, image analysis, and flow cytometry
276 [46–50]. These challenges include high variability, difficulty interpreting results across multiple metrics,
277 and reproducibility – problems that are only exacerbated when examining complex/emergent phenomena
278 that may be difficult to quantify otherwise, such as neuronal network function. While we developed and
279 validated NAS using MEA data, many of the solutions posed for the aforementioned techniques also

280 utilized PCA and other dimensionality reduction methods, suggesting a similar index scoring approach
281 may be useful for these, and other, applications to gain a deeper understanding of important results.

282

283 **Methods**

284 **Cell culture**

285 Mouse HBG3 embryonic stem cell-derived mixed neuronal and glial cells (ArunA Bio, Athens, GA) were
286 cultured according to previously published protocols [11]. Briefly, cells were thawed and seeded on
287 polyethyleneimine (Sigma Aldrich, St. Louis, MO) and laminin (Sigma)-coated MEA plates (Axion
288 Biosystems, Atlanta, GA) in 6 μ L droplets centered over the electrode grids at 40-80,000 cells/well. Cells
289 were maintained with media changes every 3-4 days with full neural culture media consisting of
290 BrainPhys™ Basal Media (STEMCELL Technologies, Vancouver, BC, Canada) or Advanced
291 DMEM/F12 (ThermoFisher, Waltham, MA) and AB2 Basal Neural Media (ArunA Bio) (1:1)
292 supplemented with 10% (v/v) KnockOut Serum Replacement (ThermoFisher), 2 mM L-glutamine
293 (ThermoFisher), 1% penicillin/streptomycin (ThermoFisher), 0.1 mM β -mercaptoethanol (Sigma), 10
294 ng/mL glial-derived neurotrophic factor (GDNF) (Peprotech Inc., Rocky Hill, NJ), and 10 ng/mL ciliary
295 neurotrophic factor (CNTF) (Peprotech).

296 BV2 microglia cells (gift from Dr. Jae-Kyung Lee, University of Georgia, Athens, GA) were cultured
297 according to previously published protocols [51]. Briefly, cells were thawed and seeded on tissue culture-
298 treated plates at approximately 5-10,000 cells/cm² and passaged at 60-80% confluency. Cells were
299 maintained with media changes every other day with neural medium consisting of DMEM/F12
300 (ThermoFisher) supplemented with 5% fetal bovine serum (FBS) (GE Healthcare, Chicago, IL), 2 mM L-
301 glutamine (ThermoFisher), and 1% penicillin/streptomycin (ThermoFisher). For lipopolysaccharide
302 (LPS) treatment, cells were treated with 10 ng/mL or 100 ng/mL LPS in neural medium for 24 hours
303 before conditioned media was collected and centrifuged to remove any cells or cellular debris.

304 **MEA preparation, recording, and data processing**

305 48-well MEA plates (Axion Biosystems) were prepared according to manufacturer's protocol. Briefly,
306 plates were coated with 0.1% polyethyleneimine (PEI) (Sigma) for 1 hour at 37°C, rinsed with sterile
307 water, and allowed to air dry in a biosafety cabinet overnight. The following day, plates were coated with
308 20 µg/mL laminin (Sigma) for 2 hours at 37°C prior to cell seeding. Mouse neural cultures (see above)
309 were seeded and allowed to adhere for 1 hour, then maintained in full neural culture media (see above)
310 supplemented with GDNF (Peprotech) and CNTF (Peprotech) (10 ng/mL each) with media changes every
311 3-4 days throughout the 3-week recording period.

312 Neuronal activity was recorded using the Maestro system (Axion Biosystems) and AxIS software v2.1-
313 2.5 (Axion Biosystems) with the following settings: band-pass filter (Butterworth, 300-5000Hz), spike
314 detector (adaptive threshold crossing, 8xSD of RMS noise), burst detector (100ms maximum inter-spike
315 interval, 5 spikes minimum, 10 spikes minimum for network bursts, 10ms mean firing rate detection
316 window). Recordings were performed daily for 2 minutes at 37°C after allowing plates to acclimate to the
317 Maestro system.

318 Raw data files were processed offline using the Statistics Compiler function in AxIS. Statistics Compiler
319 output files were processed in Microsoft Excel (Microsoft Corporation, Redmond, WA) and with custom
320 Python scripts to organize and extract individual parameter data for each well of each MEA plate and for
321 data normalization.

322 **Neural activity score calculation**

323 After initial data processing, normalization (to z-score values), and outlier removal ($-3 > z > 3$), JMP 14
324 (SAS Institute, Cary, NC) was used to conduct principal component analysis. All parameters (S1 Table)
325 were used for all wells (replicates) at 5-19 days *in vitro* (DIV). The first two principal components were
326 used to visually analyze the temporal separation of the data (Fig 2A), then the first principal component
327 was used for linear regression analysis to determine the extent of correlation to time. Finally, the factor

328 loadings for the first principal component were calculated to show the extent of contribution for each
329 individual MEA activity parameter (Table 1).

330 Factor loadings for principal component 1 were then implemented as coefficients in a formula
331 incorporating, and ultimately consolidating, all of the measured individual MEA parameters into an
332 individual index score – NAS – defined as the sum of each measured parameter value multiplied by its
333 factor loading value for each well (replicate) at each time point (Equation 1).

$$334 \quad \text{Neural activity score (NAS)} = \sum_{i=1}^n \beta_i x_i \quad (1)$$

335 *Equation 1 – where β_i are the factor loading values and x_i are the z-normalized measured values for each*
336 *parameter*

337 **Analysis of DNT hazard screening data**

338 Raw MEA data (*.raw files generated via the Maestro system and AxIS software (Axion Biosystems), see
339 above) from previous studies [21,22] was processed through the same analysis pipeline described above.

340 Additional processing for neurotoxicity data was based on methods described by Shafer et al. [21],
341 including area under curve (AUC) calculation, Hill function fitting, and EC₅₀ extrapolation. Specifically,
342 AUC values for each compound and concentration were calculated in Python 3 using the trapezoidal rule
343 (numpy.trapz() function) to integrate normalized NAS values over time (see Data Availability below for
344 more information about custom Python codes). Concentration-response curves (NAS AUC vs.
345 concentration) were generated via nonlinear least squares regression ([Inhibitor] vs. normalized response
346 model) in GraphPad Prism 8.2.0 (GraphPad Software Inc., San Diego, CA) for each compound with Hill
347 slope = -1.0, and EC₅₀ values were extrapolated from the resulting curves.

348 EC₅₀ values corresponding to cytotoxicity (Table S2) that were used for sensitivity analysis were reported
349 from previous studies [21,22]. EC₅₀ values for NAS and average MEA parameter were calculated as
350 described above.

351 **Statistical analysis**

352 Statistical analysis was performed in GraphPad Prism 8.2.0 (GraphPad Software Inc). Two-way repeated
353 measures analysis of variance (ANOVA) was used to assess differences between treatment groups over
354 time for validation studies unless otherwise noted, and post-hoc tests are stated for individual
355 experiments.

356 **Data availability**

357 Custom Python codes and MEA data (.csv files from AxIS Statistics Compiler, compiled into .xlsx file,
358 and analyzed data at several steps) are provided at the following repository:

359 <https://doi.org/10.5281/zenodo.3939310>

360

361 **Acknowledgments**

362 The authors would like to thank Dr. Tim Shafer and Dr. Katie Paul-Friedman from the Environmental
363 Protection Agency for sharing data and providing advice on toxicological analysis. The authors would
364 also like to thank Dr. Jae-Kyung Lee at the University of Georgia for providing BV2 cells.

365

366 **References**

- 367 1. Obien MEJ, Deligkaris K, Bullmann T, Bakkum DJ, Frey U. Revealing neuronal function through
368 microelectrode array recordings. *Frontiers in Neuroscience*. Frontiers Media S.A.; 2015. p. 423.
369 doi:10.3389/fnins.2014.00423
- 370 2. Johnstone AFM, Gross GW, Weiss DG, Schroeder OHU, Gramowski A, Shafer TJ.
371 Microelectrode arrays: A physiologically based neurotoxicity testing platform for the 21st century.

- 372 Neurotoxicology. 2010;31: 331–350. doi:10.1016/j.neuro.2010.04.001
- 373 3. Cotterill E, Hall D, Wallace K, Mundy WR, Eglen SJ, Shafer TJ. Characterization of Early
374 Cortical Neural Network Development in Multiwell Microelectrode Array Plates. J Biomol
375 Screen. 2016;21: 510–9. doi:10.1177/1087057116640520
- 376 4. Chiappalone M, Vato A, Tedesco M, Marcoli M, Davide F, Martinoia S. Networks of neurons
377 coupled to microelectrode arrays: A neuronal sensory system for pharmacological applications.
378 Biosensors and Bioelectronics. Elsevier Ltd; 2003. pp. 627–634. doi:10.1016/S0956-
379 5663(03)00041-1
- 380 5. Black BJ, Atmaramani R, Pancrazio JJ. Spontaneous and Evoked Activity from Murine Ventral
381 Horn Cultures on Microelectrode Arrays. Front Cell Neurosci. 2017;11: 1–10.
382 doi:10.3389/fncel.2017.00304
- 383 6. Robinette BL, Harrill JA, Mundy WR, Shafer TJ. In vitro assessment of developmental
384 neurotoxicity: Use of microelectrode arrays to measure functional changes in neuronal network
385 ontogeny. Front Neuroeng. 2011; 1–9. doi:10.3389/fneng.2011.00001
- 386 7. Strickland JD, Martin MT, Richard AM, Houck KA, Shafer TJ. Screening the ToxCast phase II
387 libraries for alterations in network function using cortical neurons grown on multi-well
388 microelectrode array (mwMEA) plates. Arch Toxicol. 2018;92: 487–500. doi:10.1007/s00204-
389 017-2035-5
- 390 8. McConnell ER, McClain MA, Ross J, LeFevre WR, Shafer TJ. Evaluation of multi-well
391 microelectrode arrays for neurotoxicity screening using a chemical training set. Neurotoxicology.
392 2012;33: 1048–1057. doi:10.1016/j.neuro.2012.05.001
- 393 9. Illes S, Fleischer W, Siebler M, Hartung HP, Dihné M. Development and pharmacological
394 modulation of embryonic stem cell-derived neuronal network activity. Exp Neurol. 2007;207:

- 395 171–176. doi:10.1016/j.expneurol.2007.05.020
- 396 10. Wagenaar DA, Pine J, Potter SM. An extremely rich repertoire of bursting patterns during the
397 development of cortical cultures. *BMC Neurosci.* 2006;7: 1–18. doi:10.1186/1471-2202-7-11
- 398 11. Wichterle H, Lieberam I, Porter JA, Jessell TM. Directed differentiation of embryonic stem cells
399 into motor neurons. *Cell.* 2002;110: 385–397. doi:10.1016/S0092-8674(02)00835-8
- 400 12. Latchoumane C-F V., Jackson L, Sendi MSE, Tehrani KF, Mortensen LJ, Stice SL, et al. Chronic
401 Electrical Stimulation Promotes the Excitability and Plasticity of ESC-derived Neurons following
402 Glutamate-induced Inhibition In vitro. *Sci Rep.* 2018;8: 10957. doi:10.1038/s41598-018-29069-3
- 403 13. Bardy C, Van Den Hurk M, Eames T, Marchand C, Hernandez R V., Kellogg M, et al. Neuronal
404 medium that supports basic synaptic functions and activity of human neurons in vitro. *Proc Natl*
405 *Acad Sci U S A.* 2015;112: E2725–E2734. doi:10.1073/pnas.1504393112
- 406 14. Aydin O, Passaro AP, Elhebeary M, Pagan-Diaz GJ, Fan A, Nuethong S, et al. Development of 3D
407 neuromuscular bioactuators. *APL Bioeng.* 2020;4: 016107. doi:10.1063/1.5134477
- 408 15. Liao B, Zhao W, Beers DR, Henkel JS, Appel SH. Transformation from a neuroprotective to a
409 neurotoxic microglial phenotype in a mouse model of ALS. *Exp Neurol.* 2012;237: 147–152.
410 doi:10.1016/J.EXPNEUROL.2012.06.011
- 411 16. Chiu IM, Morimoto ETA, Goodarzi H, Liao JT, O’Keeffe S, Phatnani HP, et al. A
412 Neurodegeneration-Specific Gene-Expression Signature of Acutely Isolated Microglia from an
413 Amyotrophic Lateral Sclerosis Mouse Model. *Cell Rep.* 2013;4: 385–401.
414 doi:10.1016/J.CELREP.2013.06.018
- 415 17. Gerber YN, Sabourin J-C, Rabano M, Vivanco M d M, Perrin FE. Early Functional Deficit and
416 Microglial Disturbances in a Mouse Model of Amyotrophic Lateral Sclerosis. Cai H, editor. *PLoS*
417 *One.* 2012;7: e36000. doi:10.1371/journal.pone.0036000

- 418 18. Frakes AE, Ferraiuolo L, Haidet-Phillips AM, Schmelzer L, Braun L, Miranda CJ, et al. Microglia
419 Induce Motor Neuron Death via the Classical NF- κ B Pathway in Amyotrophic Lateral Sclerosis.
420 Neuron. 2014;81: 1009–1023. doi:10.1016/J.NEURON.2014.01.013
- 421 19. Dunlop J, Bowlby M, Peri R, Vasilyev D, Arias R. High-throughput electrophysiology: An
422 emerging paradigm for ion-channel screening and physiology. Nat Rev Drug Discov. 2008;7:
423 358–368. doi:10.1038/nrd2552
- 424 20. Shafer TJ. Application of Microelectrode Array Approaches to Neurotoxicity Testing and
425 Screening. Advances in Neurobiology. Springer New York LLC; 2019. pp. 275–297.
426 doi:10.1007/978-3-030-11135-9_12
- 427 21. Shafer TJ, Brown JP, Lynch B, Davila-Montero S, Wallace K, Friedman KP. Evaluation of
428 Chemical Effects on Network Formation in Cortical Neurons Grown on Microelectrode Arrays.
429 Toxicol Sci. 2019;169: 436–455. doi:10.1093/toxsci/kfz052
- 430 22. Frank CL, Brown JP, Wallace K, Mundy WR, Shafer TJ. From the Cover: Developmental
431 Neurotoxicants Disrupt Activity in Cortical Networks on Microelectrode Arrays: Results of
432 Screening 86 Compounds During Neural Network Formation. Toxicol Sci. 2017;160: 121–135.
433 doi:10.1093/toxsci/kfx169
- 434 23. Brown JP, Hall D, Frank CL, Wallace K, Mundy WR, Shafer TJ. Evaluation of a microelectrode
435 array-based assay for neural network ontogeny using training set chemicals. Toxicol Sci.
436 2016;154: 126–139. doi:10.1093/toxsci/kfw147
- 437 24. Bal-Price A, Pistollato F, Sachana M, Bopp SK, Munn S, Worth A. Strategies to improve the
438 regulatory assessment of developmental neurotoxicity (DNT) using in vitro methods. Toxicol
439 Appl Pharmacol. 2018;354: 7–18. doi:10.1016/j.taap.2018.02.008
- 440 25. Nosek BA, Alter G, Banks GC, Borsboom D, Bowman SD, Breckler SJ, et al. Promoting an open

- 441 research culture. *Science* (80-). 2015;348: 1422 LP – 1425. doi:10.1126/science.aab2374
- 442 26. Begley CG, Ellis LM. Raise standards for preclinical cancer research. *Nature*. 2012;483: 531–533.
443 doi:10.1038/483531a
- 444 27. Reality check on reproducibility. *Nature*. 2016;533: 437. doi:10.1038/533437a
- 445 28. Harrill JA, Freudenrich TM, Machacek DW, Stice SL, Mundy WR. Quantitative assessment of
446 neurite outgrowth in human embryonic stem cell-derived hN2TM cells using automated high-
447 content image analysis. *Neurotoxicology*. 2010;31: 277–290. doi:10.1016/j.neuro.2010.02.003
- 448 29. de Groot MWGDM, Westerink RHS, Dingemans MML. Don't judge a neuron only by its cover:
449 Neuronal function in in vitro developmental neurotoxicity testing. *Toxicol Sci*. 2012;132: 1–7.
450 doi:10.1093/toxsci/kfs269
- 451 30. Bal-Price AK, Hogberg HT, Buzanska L, Lenas P, van Vliet E, Hartung T. In vitro developmental
452 neurotoxicity (DNT) testing: Relevant models and endpoints. *Neurotoxicology*. 2010;31: 545–554.
453 doi:10.1016/j.neuro.2009.11.006
- 454 31. Cedarbaum JM, Stambler N, Malta E, Fuller C, Hilt D, Thurmond B, et al. The ALSFRS-R: A
455 revised ALS functional rating scale that incorporates assessments of respiratory function. *J Neurol*
456 *Sci*. 1999;169: 13–21. doi:10.1016/S0022-510X(99)00210-5
- 457 32. UPDRS - Parkinson's Disease Research, Education and Clinical Centers. [cited 27 Apr 2020].
458 Available: <https://www.parkinsons.va.gov/resources/UPDRS.asp>
- 459 33. Broderick JP, Adeoye O, Elm J. Evolution of the Modified Rankin Scale and Its Use in Future
460 Stroke Trials. *Stroke*. Lippincott Williams and Wilkins; 2017. pp. 2007–2012.
461 doi:10.1161/STROKEAHA.117.017866
- 462 34. Spellicy SE, Kaiser EE, Bowler MM, Jurgielewicz BJ, Webb RL, West FD, et al. Neural Stem
463 Cell Extracellular Vesicles Disrupt Midline Shift Predictive Outcomes in Porcine Ischemic Stroke

- 464 Model. *Transl Stroke Res.* 2019; 1–13. doi:10.1007/s12975-019-00753-4
- 465 35. NINDS Know Stroke Campaign - NIH Stroke Scale. [cited 27 Apr 2020]. Available:
466 <https://www.stroke.nih.gov/resources/scale.htm>
- 467 36. Law CJ, Ashcroft HA, Zheng W, Sexton JZ. Assay development and multivariate scoring for
468 high-content discovery of chemoprotectants of endoplasmic-reticulum-stress-mediated amylin-
469 induced cytotoxicity in pancreatic beta cells. *Assay Drug Dev Technol.* 2014;12: 375–384.
470 doi:10.1089/adt.2014.591
- 471 37. Yadav B, Pemovska T, Szwajda A, Kuleskiy E, Kontro M, Karjalainen R, et al. Quantitative
472 scoring of differential drug sensitivity for individually optimized anticancer therapies. *Sci Rep.*
473 2014;4: 1–10. doi:10.1038/srep05193
- 474 38. Rotroff DM, Martin MT, Dix DJ, Filer DL, Houck KA, Knudsen TB, et al. Predictive endocrine
475 testing in the 21st century using in vitro assays of estrogen receptor signaling responses. *Environ*
476 *Sci Technol.* 2014;48: 8706–8716. doi:10.1021/es502676e
- 477 39. Geiss KT, Frazier JM, Dodd DE. Toxicity Screening of Halogenated Aliphatics Using a Novel In
478 Vitro Volatile Chemical Exposure System. NIST Special Publication. 2001.
- 479 40. Replacing the replacements: Animal model alternatives | Science | AAAS. [cited 27 Apr 2020].
480 Available: [https://www.sciencemag.org/features/2018/10/replacing-replacements-animal-model-](https://www.sciencemag.org/features/2018/10/replacing-replacements-animal-model-alternatives)
481 [alternatives](https://www.sciencemag.org/features/2018/10/replacing-replacements-animal-model-alternatives)
- 482 41. Nicklas WJ, Youngster SK, Kindt MV, Heikkila RE. IV. MPTP, MPP+ and mitochondrial
483 function. *Life Sci.* 1987;40: 721–729. doi:10.1016/0024-3205(87)90299-2
- 484 42. Miguez M, Reeve C, Wood PM, Hollomon DW. Alternative oxidase reduces the sensitivity
485 of *Mycosphaerella graminicola* to QOI fungicides. *Pest Manag Sci.* 2004;60: 3–7.
486 doi:10.1002/ps.837

- 487 43. Lin MT, Beal MF. Mitochondrial dysfunction and oxidative stress in neurodegenerative diseases.
488 Nature. Nature Publishing Group; 2006. pp. 787–795. doi:10.1038/nature05292
- 489 44. Johri A, Beal MF. Mitochondrial dysfunction in neurodegenerative diseases. Journal of
490 Pharmacology and Experimental Therapeutics. American Society for Pharmacology and
491 Experimental Therapeutics; 2012. pp. 619–630. doi:10.1124/jpet.112.192138
- 492 45. Golpich M, Amini E, Mohamed Z, Azman Ali R, Mohamed Ibrahim N, Ahmadiani A.
493 Mitochondrial Dysfunction and Biogenesis in Neurodegenerative diseases: Pathogenesis and
494 Treatment. CNS Neurosci Ther. 2017;23: 5–22. doi:10.1111/cns.12655
- 495 46. Kozak K, Seeliger J, Gedrange T. Multiparametric Analysis of High Content Screening Data. J
496 Biomed. 2017;2: 78–88. doi:10.7150/jbm.17341
- 497 47. Abraham Y, Zhang X, Parker CN. Multiparametric Analysis of Screening Data. J Biomol Screen.
498 2014;19: 628–639. doi:10.1177/1087057114524987
- 499 48. Caicedo JC, Cooper S, Heigwer F, Warchal S, Qiu P, Molnar C, et al. Data-analysis strategies for
500 image-based cell profiling. Nat Methods. 2017;14: 849–863. doi:10.1038/nmeth.4397
- 501 49. Kvistborg P, Gouttefangeas C, Aghaeepour N, Cazaly A, Chattopadhyay PK, Chan C, et al.
502 Thinking Outside the Gate: Single-Cell Assessments in Multiple Dimensions. Immunity. Cell
503 Press; 2015. pp. 591–592. doi:10.1016/j.immuni.2015.04.006
- 504 50. Takahashi T. Efficient Interpretation of Multiparametric Data Using Principal Component
505 Analysis as an Example of Quality Assessment of Microalgae. Multidimensional Flow Cytometry
506 Techniques for Novel Highly Informative Assays. InTech; 2018. doi:10.5772/intechopen.71460
- 507 51. Lee J-K, Chung J, McAlpine FE, Tansey MG. Regulator of G-protein signaling-10 negatively
508 regulates NF- κ B in microglia and neuroprotects dopaminergic neurons in hemiparkinsonian rats. J
509 Neurosci. 2011;31: 11879–88. doi:10.1523/JNEUROSCI.1002-11.2011

510 **Figures**

511 **Fig 1. Neural network ontogeny revealed by microelectrode array.** (A-F) Representative raster plots
512 of one well over time, demonstrating qualitative network development. Each plot is 5 seconds for
513 sufficient spike and burst resolution, and horizontal rows correspond to one channel/electrode, each. Note
514 the changes over time: few spikes on few channels (DIV 8) to more spikes on more channels (DIV 10) to
515 sporadic bursts (DIV 13, 16) to rhythmic network bursts (DIV 19) to stronger, rhythmic network bursts
516 (DIV 28). (G-N) Line graphs of 8 example individual MEA parameters covering major categories
517 (activity, bursting, network bursting, synchrony).

518 **Fig 2. Principal component analysis of MEA parameters reveals temporal correlation.** (A) The first
519 two principal components (accounting for 66.9% of total variation), colored by time (yellow > green >
520 blue > purple), showing a distinct pattern of separation/progression. (B) Principal component 1 (PC1) is
521 positively correlated with time. Linear regression analysis confirms this strong correlation ($R^2 = 0.5541$, F
522 = 1487, $p < 0.0001$).

523 **Fig 3. Enhancement of neural network ontogeny is easily quantified using neural activity score.** (A)
524 BrainPhys™-based culture media results in clear enhancement of neural activity compared to traditional
525 DMEM/Neurobasal-based media, and this enhancement is quantifiable via NAS ($p < 0.0001$, two-way
526 repeated measures ANOVA, $n = 24$ /group). (B) Muscle-conditioned media treatment results in similar
527 enhancement of neural activity ($p < 0.0001$, two-way repeated measures ANOVA, $n = 12$ /group).

528 **Fig 4. Disruption of neural network ontogeny is easily quantified using neural activity score.** (A)
529 Co-culturing mixed neural cultures and microglia (BV2 cells) results in a microglia concentration-
530 dependent disruption of neural activity ($p < 0.0001$, two-way repeated measures ANOVA, Tukey's post-
531 hoc test, $n = 6$ /group). (B) Similarly, BV2-conditioned media treatment resulted in a similar decrease
532 ($p < 0.0193$, two-way mixed ANOVA, Tukey's post-hoc test). Additionally, 24-hour LPS treatment of
533 BV2s prior to conditioned media collection exacerbated this disruption in a concentration-dependent

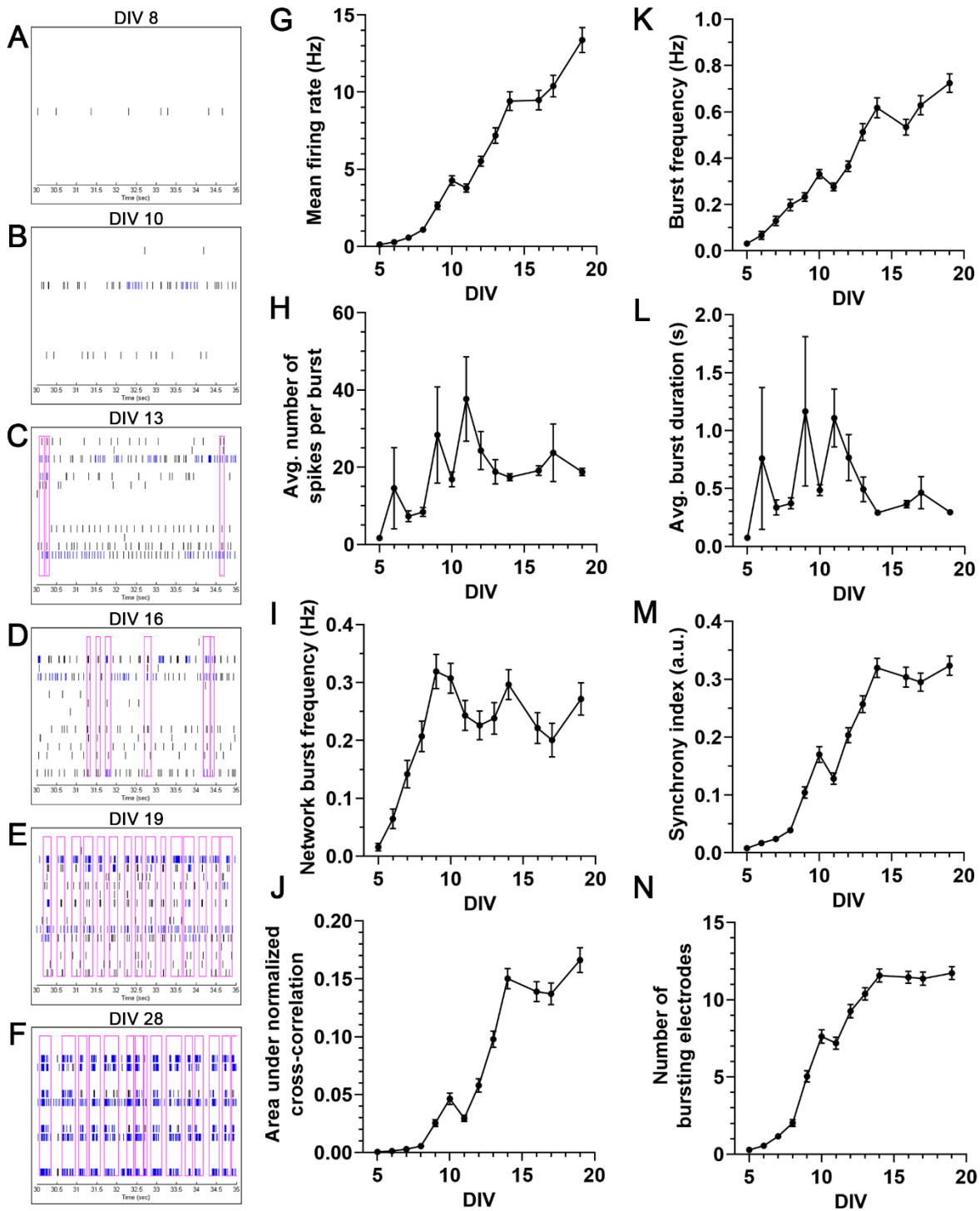
534 manner (10 ng/mL, $p=0.0003$; 100 ng/mL, $p<0.0001$) ($n=14$ /group except media control group, for which
535 $n=12$). Grey dashed lines indicate time of BV2 or CM addition. Reported statistics are Tukey's post-hoc
536 comparisons 24 hours post-addition. Connecting letters on graphs indicate comparisons for other time
537 points.

538 **Fig 5. Neural activity score summarizes neural activity for neurotoxicology screening.** (A-C)

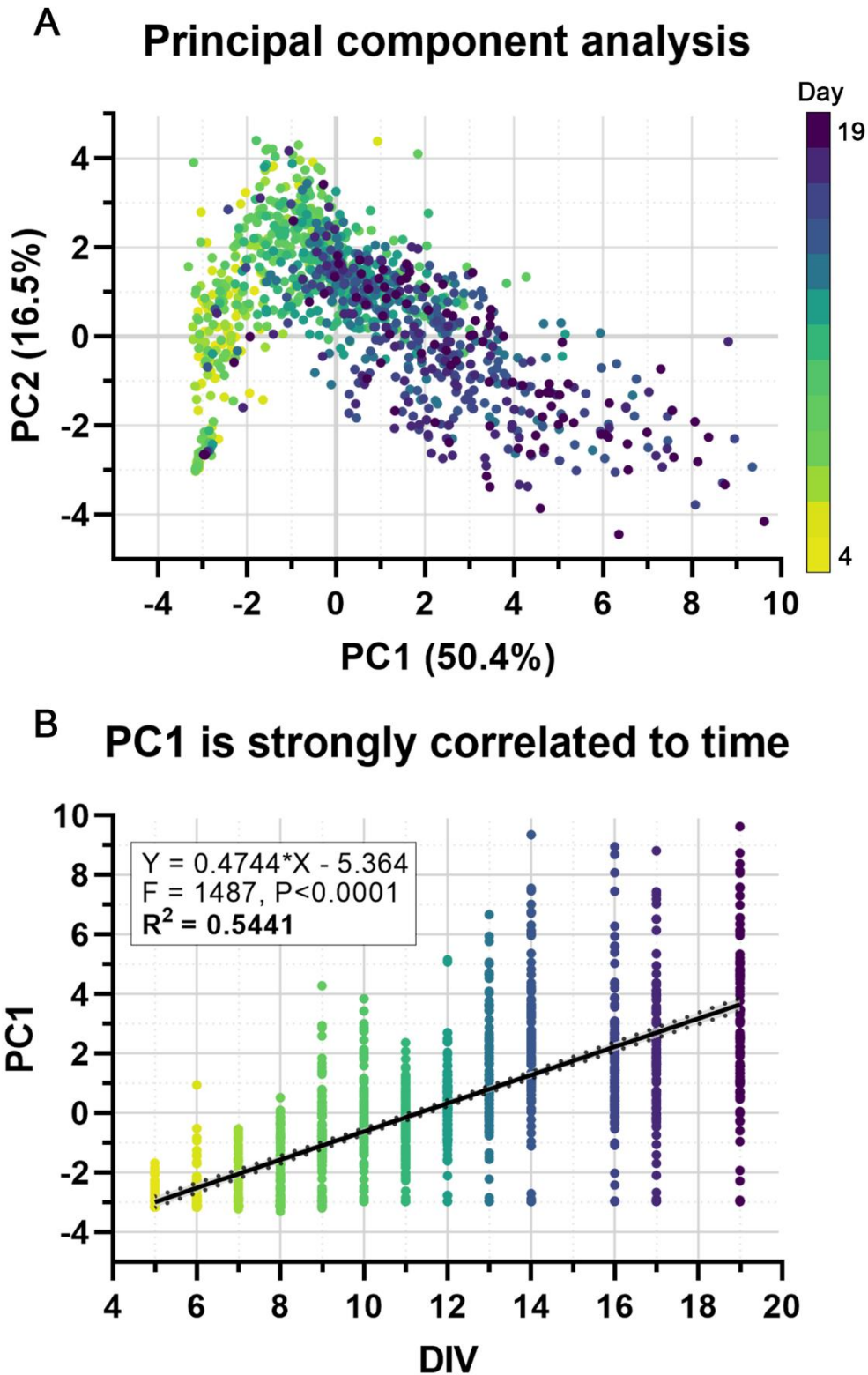
539 Examples of NAS calculation for all concentrations of three compounds of varying toxicity from EPA
540 compound libraries analyzed. (D-F) Concentration-response curves showing how EC_{50} was determined
541 for the same three compounds. Grey dotted line indicates 50% of control NAS AUC, used as a threshold
542 for EC_{50} extrapolation (indicated via red dashed line). Note the lack of extrapolation for aspirin since
543 sufficient effect was not detected. (G) Summary of NAS EC_{50} values from Frank et al. 2017 [22] and
544 Shafer et al. 2019 [21]. (Left) Total compounds with detected effects (EC_{50} within tested range). (Inset)
545 Sensitivity comparisons for NAS vs. average individual MEA parameter and cytotoxicity assays for all
546 compounds with detected effects. Higher sensitivity is defined as lower EC_{50} value.

547

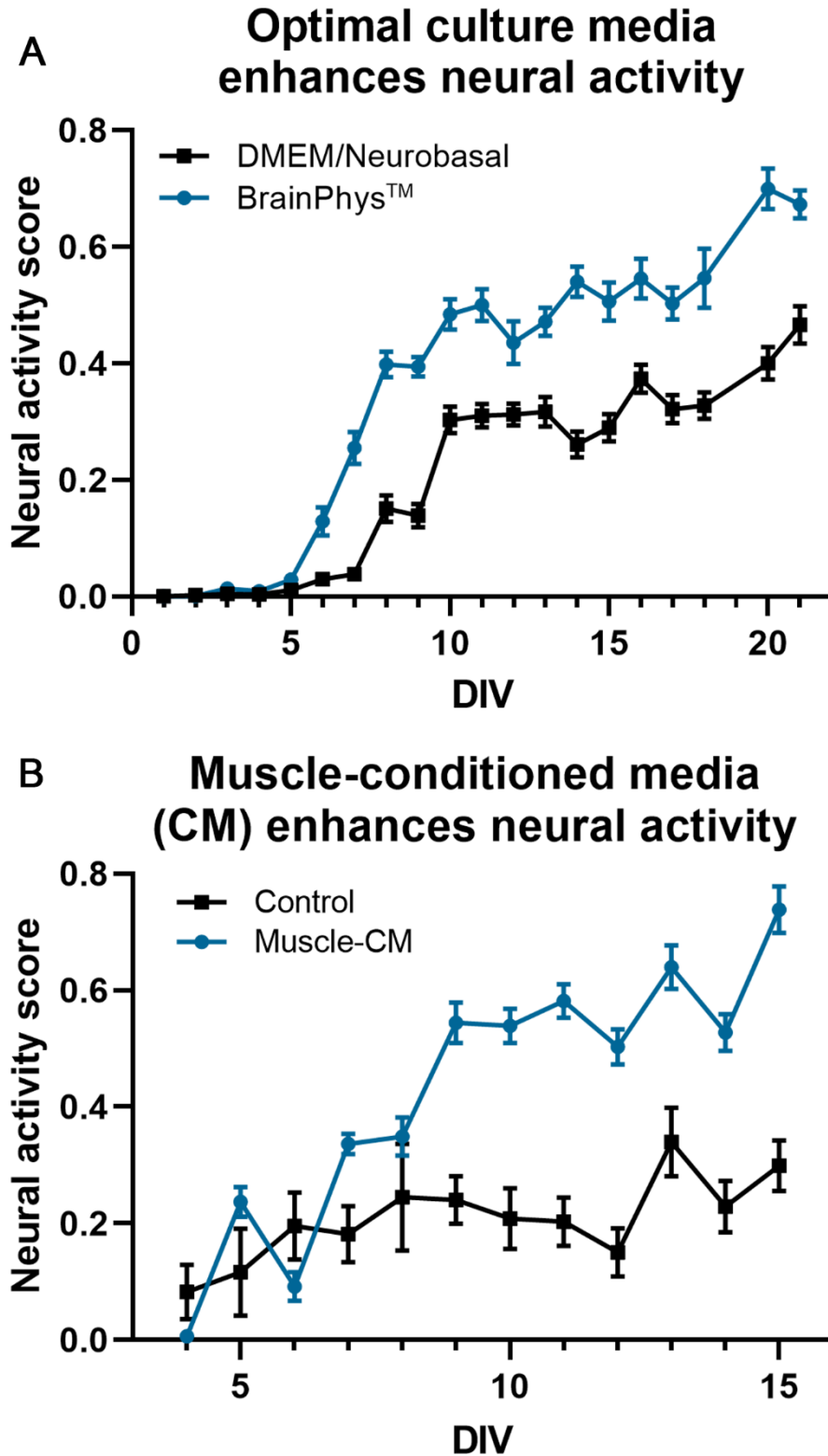
548 **Figure 1. Neural network ontogeny revealed by microelectrode array.**



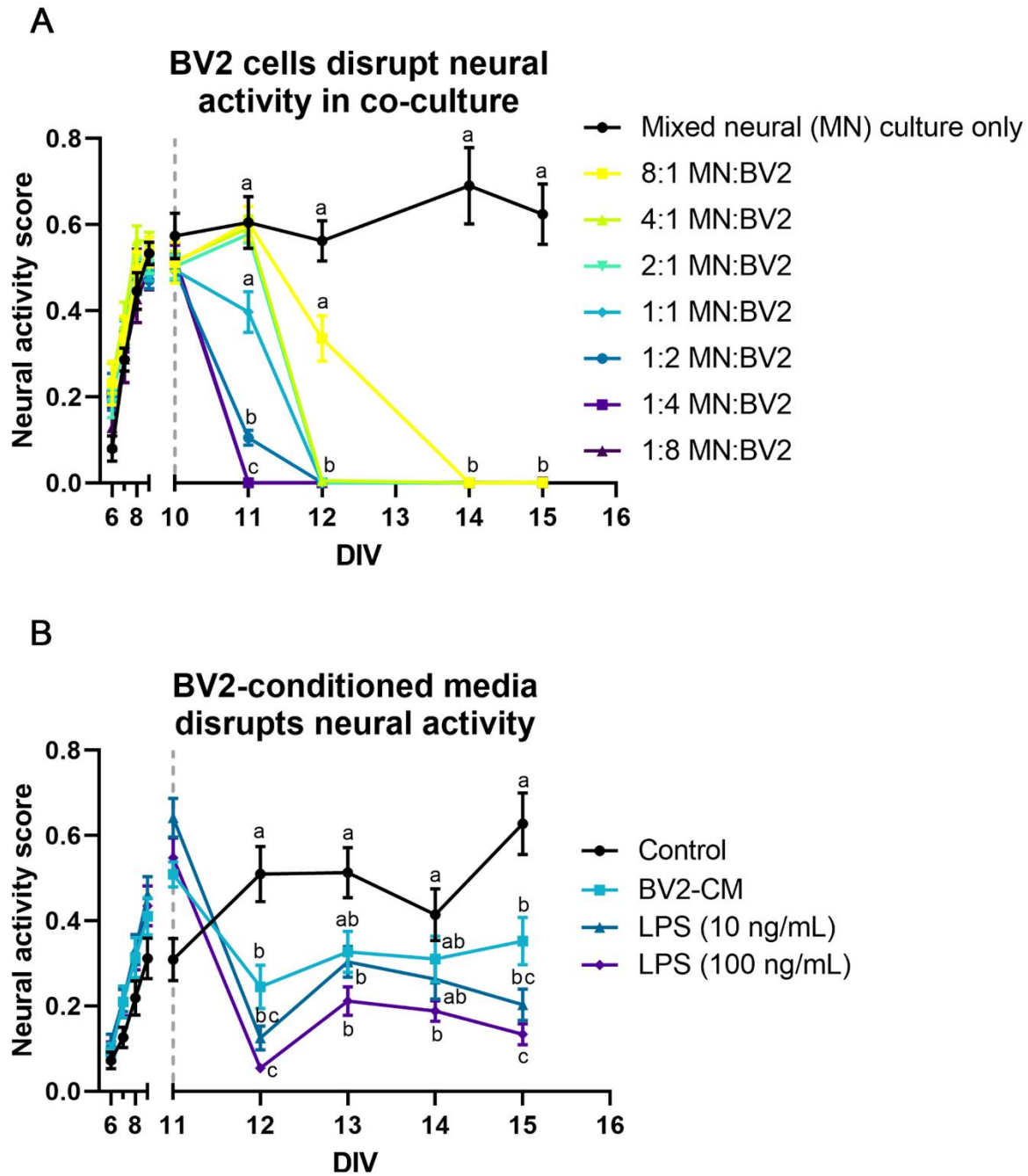
550 **Figure 2. Principal component analysis of MEA parameters reveals temporal correlation.**



552 **Figure 3. Enhancement of neural network ontogeny is easily quantified using neural activity score.**



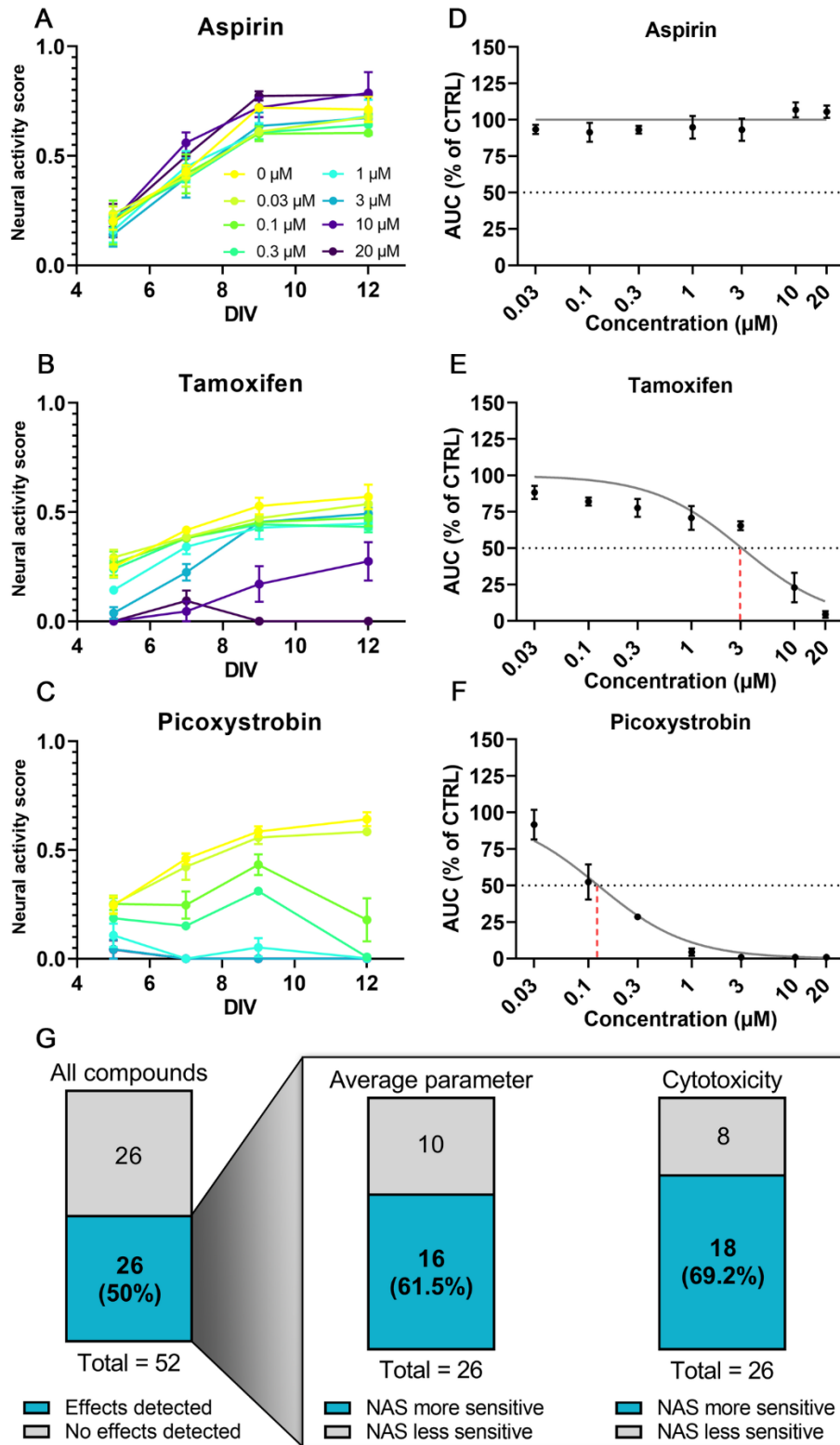
554 **Figure 4. Disruption of neural network ontogeny is easily quantified using neural activity score.**



555

556

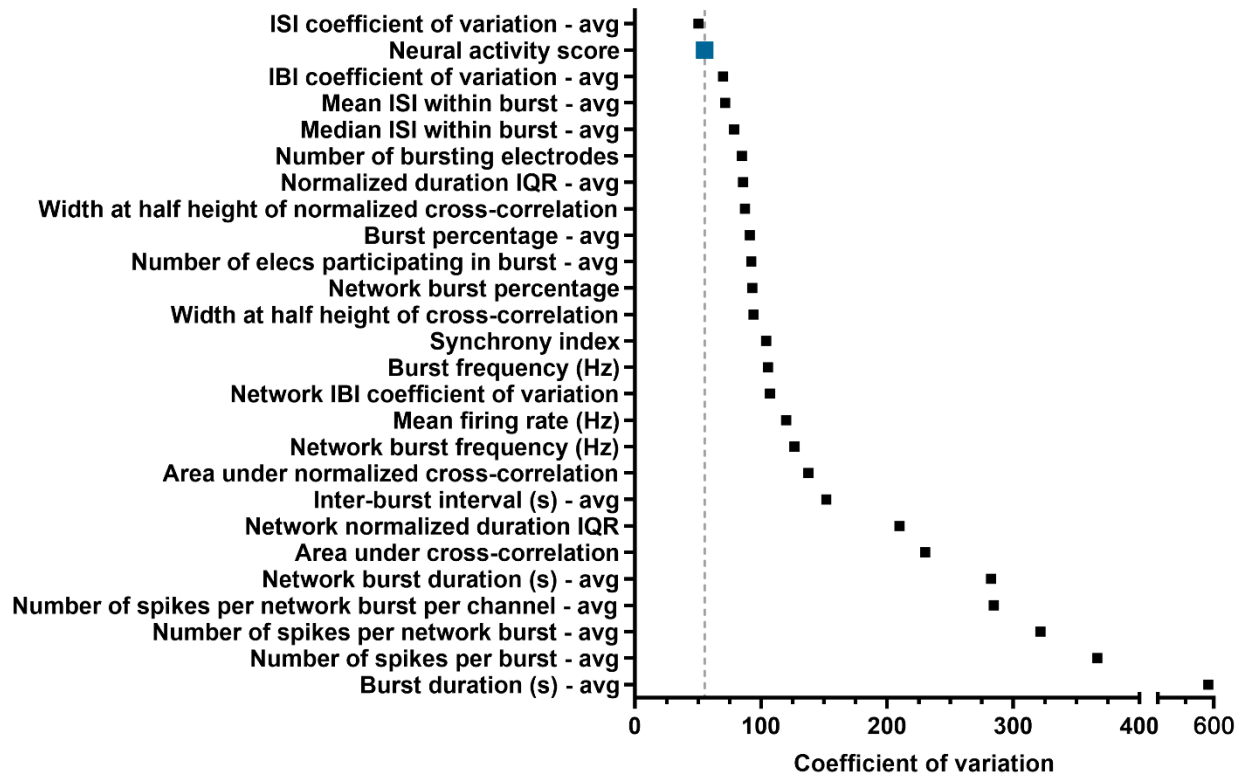
557 **Figure 5. Neural activity score summarizes neural activity for neurotoxicology screening.**



559 **Supporting information**

560 **S1 Fig. Coefficient of variation values for all individual parameters and neural activity score.**

561 Values were calculated from network ontogeny data (Fig 1).



562

563

564 **S1 Table. List of all MEA parameters analyzed.**

<i>Parameter name</i>
Mean firing rate (Hz)
Inter-spike interval (ISI) coefficient of variation – Avg
Number of bursting electrodes
Burst duration – Avg (s)
Number of spikes per burst
Mean ISI within burst – Avg
Median ISI within burst – Avg
Inter-burst (IBI) interval – Avg
Burst frequency (Hz)
Normalized burst duration IQR – Avg
IBI coefficient of variation – Avg
Burst percentage – Avg
Network burst frequency (Hz)
Network burst duration – Avg (s)
Number of spikes per network burst – Avg
Number of electrodes participating in burst – Avg
Number of spikes per network burst per channel – Avg
Network burst percentage
Network IBI coefficient of variation
Network normalized duration IQR
Area under normalized cross-correlation
Area under cross-correlation
Width at half height of normalized cross-correlation

Width at half height of cross-correlation

Synchrony index

565

566

S2 Table. EC₅₀ values for all compounds analyzed in EPA network formation and toxicity assays. Values were calculated from neural activity score, minimum individual parameter, average of all parameters, and cytotoxicity.

<i>Compound</i>	<i>CASRN</i>	<i>EC₅₀ (μM)</i>		
		<i>Neural activity score</i>	<i>Avg. individual MEA parameter</i>	<i>Avg. cytotoxicity</i>
1-Methyl-4-phenylpyridinium iodide	36913-39-0	4.93	4.88	6.5483
1-Ethyl-3-methylimidazolium diethylphosphate	848641-69-0	N/A	N/A	N/A
3-Iodo-2-propynyl-N-butylcarbamate	55406-53-6	2.42	3.13	3.03535
6 Propyl 2 thiouracil	51-52-5	N/A	N/A	N/A
Abamectin	71751-41-2	0.16	0.37	3.9339
Acenaphthene	83-32-9	N/A	N/A	N/A
Aldrin	309-00-2	4.14	4.26	7.30305
Aspirin	50-78-2	N/A	N/A	N/A
Atrazine	1912-24-9	N/A	N/A	N/A
Auramine O	2465-27-2	2.49	3.00	3.50965
Benz(a)anthracene	56-55-3	N/A	N/A	N/A
Berberine chloride	633-65-8	1.83	2.03	0.2499
Bisphenol AF	1478-61-1	N/A	N/A	16.46775

Bisphenol B	77-40-7	N/A	N/A	N/A
Boric acid	10043-35-3	N/A	N/A	N/A
Boscalid	188425-85-6	N/A	N/A	N/A
Carbamic acid, butyl-, 3-iodo-2-propynyl ester	55406-53-6	1.42	1.43	1.22425
Chlordane	57-74-9	5.86	5.63	5.7725
Cloprop	101-10-0	N/A	N/A	N/A
Clove leaf oil	8000-34-8	N/A	N/A	N/A
D-Glucitol	50-70-4	N/A	N/A	N/A
Diphenhydramine hydrochloride	147-24-0	18.12	11.56	N/A
Disulfiram	97-77-8	0.85	0.64	0.0954
Endosulfan	115-29-7	8.71	8.84	8.90985
Endrin	72-20-8	N/A	N/A	N/A
Erythromycin	114-07-8	N/A	N/A	N/A
Estradiol	50-28-2	N/A	N/A	N/A
Eugenol	97-53-0	N/A	N/A	N/A
Fenamiphos	22224-92-6	N/A	N/A	N/A
Fluoxastrobin	361377-29-9	0.69	0.89	1.1693
Glycerol	56-81-5	N/A	N/A	N/A

Hexachlorophene	70-30-4	1.92	1.83	1.8547
Kepone	143-50-0	5.91	5.39	8.1115
L-Ascorbic acid	50-81-7	N/A	N/A	N/A
Mancozeb	8018-01-7	N/A	N/A	N/A
Manganese, tricarbonyl[(1,2,3,4,5-.eta.)-1- methyl-2,4-cyclopentadien-1-yl]	12108-13-3	N/A	N/A	N/A
Methoxychlor	72-43-5	7.45	8.51	8.26275
MGK 264	113-48-4	N/A	N/A	N/A
Mirex	2385-85-5	3.81	4.36	2.8233
o,p'-DDT	789-02-6	4.14	4.09	5.10525
Parathion	56-38-2	N/A	N/A	N/A
Permethrin	52645-53-1	6.16	7.83	10.45295
Picoxystrobin	117428-22-5	0.13	0.32	0.5449
Piperonyl butoxide	51-03-6	N/A	N/A	19.1251
pp-DDD	72-54-8	4.83	4.60	6.0773
pp-DDE	72-55-9	4.50	4.33	4.606
pp-DDT	50-29-3	4.36	4.33	4.0716
Reserpine	50-55-5	1.31	1.68	9.08055

Rotenone	83-79-4	0.41	0.64	0.03005
Tamoxifen	10540-29-1	3.09	4.35	6.4836
Tetracycline	60-54-8	N/A	N/A	N/A
Triclosan	3380-34-5	9.08	9.91	9.21815

567 N/A indicates EC₅₀ not determined within range (0-20 μ M). Individual parameter averages were only calculated if 13+ (>50%) parameters had
568 determinable ($0 < EC_{50} < 20$) values. Bolded NAS values indicate compounds where NAS was more sensitive (lower EC₅₀) than the avg.
569 individual parameter value.